Systems/Circuits

A Short Route for Reach Planning between Human V6A and the Motor Cortex

Rossella Breveglieri,[1] Sara Borgomaneri,[2,3] Stefano Diomedi,[1] Alessia Tessari,[4] Claudio Galletti,[1] and Patrizia Fattori[1,5]

[1]Department of Biomedical and Neuromotor Sciences, University of Bologna, 40126 Bologna, Italy, [2]Center for studies and research in Cognitive Neuroscience, University of Bologna, 47521 Cesena, Italy, [3]Istituto di Ricovero e Cura a Carattere Scientifico (IRCCS) Santa Lucia Foundation, 00179 Rome, Italy, [4]Department of Psychology "Renzo Canestrari", University of Bologna, 40127 Bologna, Italy, and [5]Alma Mater Research Institute for Human-Centered Artificial Intelligence (Alma Human AI), University of Bologna, 40126 Bologna, Italy

In the macaque monkey, area V6A, located in the medial posterior parietal cortex, contains cells that encode the spatial position of a reaching target. It has been suggested that during reach planning this information is sent to the frontal cortex along a parieto-frontal pathway that connects V6A–premotor cortex–M1. A similar parieto-frontal network may also exist in the human brain, and we aimed here to study the timing of this functional connection during planning of a reaching movement toward different spatial positions. We probed the functional connectivity between human area V6A (hV6A) and the primary motor cortex (M1) using dual-site, paired-pulse transcranial magnetic stimulation with a short (4 ms) and a longer (10 ms) interstimulus interval while healthy participants (18 men and 18 women) planned a visually-guided or a memory-guided reaching movement toward positions located at different depths and directions. We found that, when the stimulation over hV6A is sent 4 ms before the stimulation over M1, hV6A inhibits motor-evoked potentials during planning of either rightward or leftward reaching movements. No modulations were found when the stimulation over hV6A was sent 10 ms before the stimulation over M1, suggesting that only short medial parieto-frontal routes are active during reach planning. Moreover, the short route of hV6A–premotor cortex–M1 is active during reach planning irrespectively of the nature (visual or memory) of the reaching target. These results agree with previous neuroimaging studies and provide the first demonstration of the flow of inhibitory signals between hV6A and M1.

Key words: **humans; inhibitions; parietofrontal network; planning; reaching; transcranial magnetic stimulation**

Significance Statement

All our dexterous movements depend on the correct functioning of the network of brain areas. Knowing the functional timing of these networks is useful to gain a deeper understanding of how the brain works to enable accurate arm movements. In this article, we probed the parieto-frontal network and demonstrated that it takes 4 ms for the medial posterior parietal cortex to send inhibitory signals to the frontal cortex during reach planning. This fast flow of information seems not to be dependent on the availability of visual information regarding the reaching target. This study opens the way for future studies to test how this timing could be impaired in different neurological disorders.

Introduction

The medial posterior parietal cortex (mPPC) is a key node of the parieto-frontal networks that transform visuospatial information about a target to be reached into motor plans (Mountcastle et al., 1975; Snyder et al., 2000; Koch et al., 2008; Vesia et al., 2013; Fattori et al., 2017; Diomedi et al., 2021; Breveglieri et al., 2021a). In the macaque, mPPC hosts area V6A (Galletti et al., 1999), which contains, among others, reach-related cells (Fattori et al., 2005, 2017; Hadjidimitrakis et al., 2014; Bosco et al., 2016; Diomedi et al., 2020). V6A has also been identified in humans [human V6A (hV6A); Pitzalis et al., 2015], and its role in reaching has been demonstrated by neuroimaging (Astafiev et al., 2003; Connolly et al., 2003; Beurze et al., 2009; Cavina-Pratesi et al., 2010; Tosoni et al., 2015) and transcranial magnetic stimulation (TMS) studies (Vesia et al., 2010; Ciavarro et al., 2013; Breveglieri et al., 2021a).

In both species, the connections between V6A and primary motor cortex (M1) are indirect through the dorsal premotor

Received June 22, 2022; revised Dec. 16, 2022; accepted Dec. 22, 2022.

Author contributions: R.B. and S.B. designed research; R.B. and S.B. performed research; R.B., S.B., S.D., and A.T. analyzed data; R.B., C.G., and P.F. wrote the paper.

This work was supported by the MAIA Project, which received funding from the European Union's Horizon 2020 research and innovation program under Grant Agreement No. 951910.

The authors declare no competing financial interests.

Correspondence should be addressed to Rossella Breveglieri at rossella.breveglieri@unibo.it.

https://doi.org/10.1523/JNEUROSCI.1609-22.2022

cortex (PMd) and, specifically, the parts of PMd and M1 involved contain a representation of the arm (Galletti et al., 2004; Gamberini et al., 2009; Passarelli et al., 2011, 2018; Tosoni et al., 2015). These pieces of evidence suggest that the functionality of this network underlies dexterous arm movements. Recently, two studies have demonstrated the timing of the connections between hV6A and M1 at rest (Vesia et al., 2013; Breveglieri et al., 2021b) using dual-site, paired-pulse TMS. In this protocol (Koch et al., 2007), a conditioning stimulus (CS) is administered over a target (e.g., parietal) area to activate direct or indirect pathways from the target site to M1. The CS is followed by a test stimulus (TS) administered over M1 to induce motor-evoked potentials (MEPs) in contralateral muscles (Koch et al., 2007; Rothwell, 2011; Fiori et al., 2016, 2017; Chiappini et al., 2020).

In our article (Breveglieri et al., 2021b), we demonstrated that hV6A sends inhibitory signals to M1 at interstimulus intervals (ISIs) of 12 or 15 ms, whereas shorter ISIs were not effective (Breveglieri et al., 2021b; but see also Vesia et al., 2013). This suggests that the exchange of information at rest between hV6A and the frontal cortex occurred not through a direct hV6A–M1 connection, but through a longer circuit that likely involved the lateral parietal cortex, ventral premotor cortex (PMv), and PMd.

A question arises in terms of whether the same timing of the parieto-frontal circuits can be found during action planning. Interestingly, corticospinal excitability was increased by a pulse over the lateral parietal cortex while preparing an immediate (i.e., without delay) contralateral reach (Koch et al., 2008) at ISIs of 4 ms (TMS over right PPC) or 6 ms (TMS over left PPC). Moving toward more medial sites, Vesia et al. (2013) similarly showed that a CS over superior parieto-occipital cortex SPOC area (also including area hV6A; see below) 4 ms before the TS in M1 facilitated the corticospinal excitability during reach or grasp planning but only when arm transport was required. These latter studies suggested that short routes from SPOC to M1 are functionally specific to arm transport.

It is of note that reaching cells of monkey V6A are spatially tuned during reach planning and execution (Fattori et al., 2005; Hadjidimitrakis et al., 2014; Bosco et al., 2016). These data have been confirmed in fMRI studies in humans (Cavina-Pratesi et al., 2010). Moreover, in a recent TMS study from our laboratory, we found that reaching accuracy is impaired in a spatial-dependent manner when interfering with single-pulse TMS over hV6A (Breveglieri et al., 2021a). Thus, it can be hypothesized that the signals sent by hV6A during reach planning could bring spatial information to M1. If this were the case, the modulation of the corticospinal excitability by hV6A would be spatial dependent. To test this hypothesis, we tested here the functional connectivity of hV6A–M1 during the planning of reaching movements directed toward targets located at different depths and directions with dual-site, paired-pulse TMS.

Materials and Methods

Participants

Thirty-six healthy volunteers, subdivided into a group of 18 participants in experiment 1 (10 men; mean age, 24.44 ± 3.91 years) and another 18 in experiment 2 (8 men; mean age, 23.89 ± 3.20 years), participated in this study. The number of participants was determined based on a power analysis that indicated that a sample size of 36 participants is an appropriate sample size to achieve statistical power ($1 - \beta$) of 0.8 (two-tailed $\alpha = 0.05$; effect size $f = 0.20$; Breveglieri et al., 2021a), analysis performed using G*Power software (Faul et al., 2007).

All participants were right handed according to the standard handedness inventory (Oldfield, 1971) and had normal or corrected-to-normal vision. None of the participants had neurologic, psychiatric, or other medical problems or any contraindication to TMS (Rossi et al., 2009; Rossini et al., 2015). Participants provided written informed consent. The procedures were approved by the Bioethical Committee at the University of Bologna (Protocol 57635) and were in accordance with the ethical standards of the Declaration of Helsinki (2013). No discomfort or adverse effects during TMS were reported or noticed.

Localization of brain sites

Before each experimental session, the positions for the coils were identified on each participant's scalp. The optimal scalp position for coil placement over the left M1 was sought on the participant's head while they were wearing a bathing cap and was defined as the point where stimulation evoked the largest MEPs from the contralateral first dorsal interosseous (FDI) muscle of the right hand. To find the position in the left hemisphere that corresponds to the coordinates of area hV6A, we used frameless stereotaxic neuronavigation before each experimental session using the SofTaxic Navigator system (E.M.S.), similarly to previous studies (Breveglieri et al., 2021a, b). In the first stage, skull landmarks (nasion, inion, and two preauricular points) and 65 points providing a uniform representation of the scalp were digitized by means of a Polaris Vicra Optical Tracking System (Northern Digital). Coordinates in Talairach space were automatically estimated by the SofTaxic Navigator from an MRI-constructed stereotaxic template. This procedure has been proven to ensure a good localization accuracy, showing an error of ~5 mm compared with methods based on individual MRIs (Carducci and Brusco, 2012).

The Talairach coordinates used for hV6A were $x = -10$, $y = -78$, and $z = 40$ (Talairach and Tournoux, 1988). These coordinates are the same as those used in previous TMS studies on hV6A (Ciavarro et al., 2013; Breveglieri et al., 2021a, b) and are similar to those used for studying the SPOC (Vesia et al., 2010, 2017), a region that has also been investigated in imaging studies (Cavina-Pratesi et al., 2010; Gallivan et al., 2011; Tosoni et al., 2015), and that likely includes hV6A (Pitzalis et al., 2013). The neuronavigation system was then used to estimate the projections of scalp sites on the brain surface. The mean coordinates ± SD corresponded to the hV6A (experiment 1: $x = -12.3 \pm 2.9$, $y = -80.8 \pm 2.8$, $z = 38.1 \pm 2.8$; experiment 2: $x = -11.8 \pm 3.2$, $y = -79.8 \pm 2.9$, $z = 39.0 \pm 2.7$).

Transcranial magnetic stimulation protocol

A dual-site, paired-pulse transcranial magnetic stimulation paradigm with two coils was used to test the connectivity between the left PPC (hV6A) and the ipsilateral (left) M1. TMS pulses were administered via two branding-iron 50 mm butterfly coils, each of which was connected to a DuoMAG MP-Dual TMS System Monophasic Transcranial Stimulator (DEYMED). To set TMS intensity, the resting motor threshold (rMT) was estimated for all participants in a preliminary phase of the experiment using standard procedures. MEPs induced by stimulation of the left motor cortex were recorded from the right FDI muscle by means of a two-channel DuoMAG MEP amplifier. Electromyography (EMG) signals were filtered with a finite impulse response filter and digitized at a sampling rate of 5 kHz. Pairs of disposable pregelled Ag–AgCl surface electrodes were placed in a belly tendon montage with a ground electrode on the midpoint of the palmar surface of the wrist. The optimal scalp position for inducing MEPs from the right FDI muscle was first localized, and the rMT was determined from that position. The rMT was defined as the minimal intensity of stimulator output that produced MEPs with an amplitude of at least 50 μV in the FDI muscle with a probability of 50% (Rossini et al., 2015). The mean rMT across participants was 45 ± 4% (experiment 1) and 45 ± 6% (experiment 2), in line with other studies (Cardellicchio et al., 2020).

TMS was administered as TS over M1, with a preceding CS over hV6A with two ISIs (4 and 10 ms). With the aim of obtaining a stable EMG signal, in the "at rest" blocks, participants were asked to keep both hands relaxed throughout the entire testing block. In the reach planning blocks, the participants were asked to keep their arms and hands relaxed until they heard the TMS sound, which represented the Go signal, cueing execution of the reaching movement.

The intensity of the TS was adjusted to elicit an MEP of 1 mV peak to peak in the relaxed right FDI muscle (Koch et al., 2007), and this

corresponded with 120% (experiment 1) and 122% (experiment 2) of the rMT across participants. The intensity of the CS stimulus was set at 90% rMT (Koch et al., 2007; Vesia et al., 2013, 2017; Fiori et al., 2016, 2017; Breveglieri et al., 2021b). Both coils were held tangentially to the skull, with the M1 coil at 45° and the hV6A coil at 90° from the mid-sagittal line to induce a posterior–anterior-directed current in the underlying cortical tissue (Vesia et al., 2013, 2017; Breveglieri et al., 2021a, b).

Electromyographic recordings

During each stimulation session, EMG was used to monitor muscle activity from FDI, abductor digiti minimi (ADM), extensor carpi radialis (ECR), and flexor carpi radialis (FCR) muscles (Borgomaneri et al., 2017). Surface electromyograms were recorded by means of a Digitimer D440-4 system (Digitimer), amplified to 1000×, bandpass filtered between 30 Hz and 1 kHz with a sample rate of 1 kHz recorded using a Micro1401 data acquisition interface controlled by Signal software (version 7; Cambridge Electronic Design) and sorted on a computer for offline analysis.

Experimental design: apparatus and behavioral task

We sought to investigate the connectivity between the left PPC (hV6A) and the ipsilateral M1 during reach planning in two different experiments. In the first one (experiment 1), participants were asked to plan and perform memory-guided reaching movements (hereafter called "memory-guided task"); in the second one (experiment 2), participants were asked to plan and perform visually-guided reaching movements (hereafter called "visually-guided" task). Both tasks were pointing tasks where participants performed reaching movements with the tip of the index finger.

The apparatus consisted of a 19 inch touchscreen (IntelliTouch 1939L, Elo) laid horizontally on a desk located at waist level, so as to present targets in different directions but also at different distances (depth) in relation to the body. The screen displayed the targets of reaching movements. Participants performed the task with their right hand. In all trials, the reaching movement began with the participant's right hand on a marked position adjacent to the touchscreen, in front of the participant's chest. A participant sat on a comfortable chair in a darkened room, and their head was kept stable using a head/chin rest to minimize head movements. The stimuli were green (fixation point; diameter, 0.3 cm) and red (reaching target; diameter, 0.6 cm) dots (Fig. 1) and had a luminance of ~17 cd/m^2. The visible display size of the touchscreen was 37.5 × 30 cm. The display had a resolution of 1152 × 864 pixels and a frame rate of 60 Hz.

The targets were positioned as shown in Figure 1*A*. The targets could appear in four possible locations arranged in a rhombus with a diagonal of 20 cm, with a central target, the fixation point (Fig. 1*A*, cross), located 39 cm away from the participants' chest along the midline: left, far, near, right (Fig. 1*A*). All targets were located within a comfortable reaching distance for all participants tested. In all trials, the position of the fixation point was not coincident with the position of the reaching target, so that all the reaching movements were peripheral. We tested peripheral reaching because this is the eye–hand configuration that appears to be the most effective for hV6A (Breveglieri et al., 2021a) and because this configuration is typically used in TMS studies on reaching in the parietal cortex (Vesia et al., 2006, 2008, 2010).

The sequence of visually-guided and memory-guided reaching was similar for the two tasks (Fig. 1*B*) and consisted of an intertrial period (Intertrial, 6 s), followed by the presentation of the fixation point on the touchscreen (Fig. 1*B*, eye). Then, the participant had to stare at the fixation point (Fixation) for a period of 1.3–1.5 s while remaining relaxed with their hand pronated on the table. After this period, the reaching target appeared (Cue) and stayed on for the remaining trial duration (Visually-guided task) or turned off after 150 ms (Memory-guided task), and this indicated to the participants the position to be subsequently reached while maintaining fixation on the fixation target. After 0.3 s from the target onset (Cue/Delay, Visually-guided task) or after 0.3 s from the target offset (Delay, Memory-guided task), the TMS was delivered, and its "click" sound was the go signal (TMS/Go) for the participant to reach the target. The participants had to maintain fixation on the fixation point throughout the trial. After touching the visualized or memorized target position (Movement offset), the fixation point switched off and a new intertrial period started. In the Visually-guided task, the target itself disappeared when touched. Participants were asked to move their hand in a ballistic manner (without pauses or interruptions), at a fast but comfortable speed, and as accurately as possible. The starting position of the reaching hand was constant across the different stimulation conditions and experiments.

Stimulations were divided into six blocks for each experiment. The first and last blocks consisted of stimulation at rest, and comprised 60 trials, 20 with a TS alone and 40 with a TS coupled with a preceding CS, 20 with an ISI of 4 and 20 with an ISI of 10 (duration of each block, 6 min). The remaining four blocks (duration, 9 min) consisted of stimulation during reach planning and comprised 60 trials each (20 TS and 20 CS-TS for each ISI). In each reaching block, the target position was randomized across participants. The order of the ISIs was compensated. A 3 min break was allowed between blocks.

For stimuli presentation and data analysis, we used MATLAB (MathWorks) with the Psychophysics toolbox extension (Brainard, 1997).

Data acquisition and statistical analysis

MEPs. The mean peak-to-peak MEP amplitude was computed for the 4 ms ISI (p-pulse4), the 10 ms ISI (p-pulse10), and the single-pulse (s-pulse) condition. To verify that the initial pre-TMS background was similar, we checked for any trace showing EMG activity 100 ms before the TMS pulses and, in each condition and experiment, for any MEPs with amplitudes deviating from the mean by >2.5 SDs. No MEPs were discarded based on this analysis.

To investigate whether the MEPs evoked by stimulation over M1 were spatially tuned, mean MEP amplitudes of s-pulse reaching trials in each experiment were submitted to a two-way ANOVA with Task as a between-participants factor (Visually-guided and Memory-guided tasks), and Position (left, far, near, right) and Muscle (FDI, ADM, ECR, FCR) as within-participants factors.

Furthermore, to quantify the paired-pulse effect (PPE) of hV6A on M1, the ratio of MEP amplitudes between single pulse and paired pulse for each individual and stimulus-onset asynchrony was indexed through *z* scores in each muscle, task, and position by calculating the PPE index (Buch et al., 2010), computed as the difference of the mean paired-pulse TMS minus the single-pulse TMS MEP magnitudes, divided by the pooled SD. The PPE is a standard measure of causal influence of one cortical area over another (Civardi et al., 2001; Koch et al., 2006b; O'Shea et al., 2007; Mars et al., 2009; Buch et al., 2010; Van Campen et al., 2013). PPE gives a value of zero in the case of no effect of hV6A pulse on the MEP amplitude and also on the excitability of the corticospinal pathway. Positive PPE values indicate that the hV6A pulse increased the excitability of the motor cortex (excitation); negative PPE values indicate that the hV6A pulse decreased the excitability of the motor cortex (inhibition). The PPE values were then submitted to an ANOVA with Task (Visually-guided and Memory-guided tasks) as a between-participants factor, and Position (left, far, near, right), Muscle (FDI, ADM, ECR, FCR), and ISI (4 ms, 10 ms) as within-participants factors. To identify the positions of reach planning in which the hV6A pulse was effective in conditioning corticospinal excitability, we tested the PPE in each position of each task, and each muscle, against zero (one-sample Student's *t* test, $p < 0.05$) as performed in the study by Van Campen et al. (2013). In the case of multiple positions in which CS was effective, we compared the PPE of these positions with a one-way ANOVA with Position as the factor ($p < 0.05$).

Kinematics. The kinematics of reaching movements were recorded using a motion-tracking system (VICON motion capture system: six Vero 2.2 cameras, 2.2 megapixels, 2048 × 1088 pixel resolution) by sampling the position of two markers at a frequency of 100 Hz; markers were attached to the wrist (on the radial styloid process) and to the tip of the right index finger. Movement onset was determined as the moment when the velocity of the markers exceeded 30 mm/s, whereas offset was defined as the moment in which velocity fell, and remained, below this threshold. The population trajectories of movements in each stimulation condition for each task are shown in Figure 1*C*.

All the ANOVAs were repeated-measures tests, and all *post hoc* tests were performed with the Bonferroni correction.

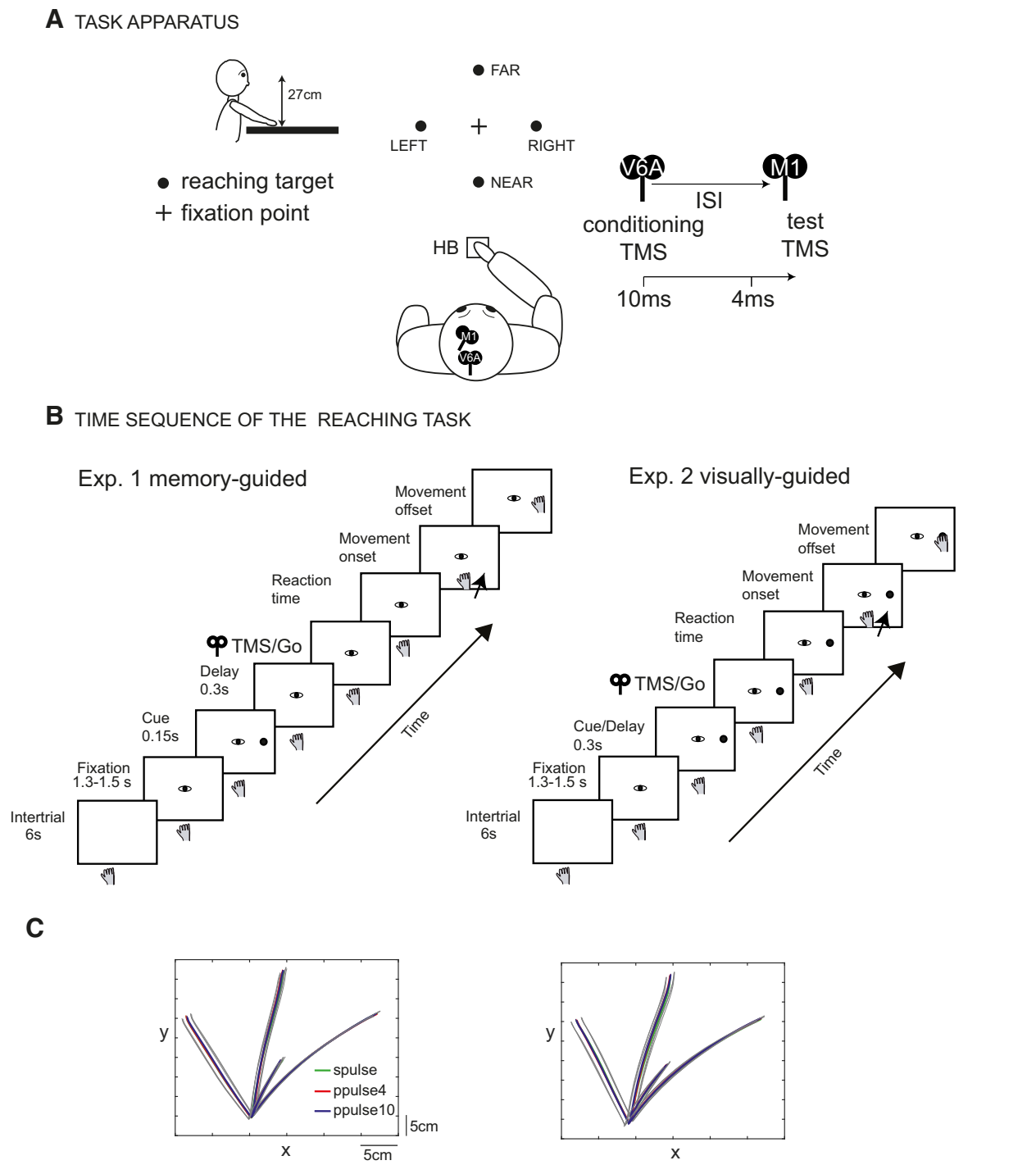

Figure 1. Experimental setup. ***A***, Lateral (left) and top (middle) views of the target arrangements in the experimental task. The participants performed reaching movements with their right hand toward one of the targets (black dots) located at different depths and directions while fixating a fixation point (cross). Reaching movements were performed from the initial hand position [home button (HB)]. Right, Schematic representation of the ISI tested in the experiments. ***B***, Time sequence of the task in experiments 1 (left) and 2 (right), where only one target position is shown for conciseness. In experiment 1, reaching was performed toward a memorized target position. In experiment 2, reaching was performed toward the visualized target position. The eye represents the fixation point, the filled black circle the reaching target. TMS was delivered after 300 ms of planning and represented the Go signal for reaching movements. ***C***, Population trajectories of the index finger during trials of experiments 1 (left) and 2 (right). Green lines, averaged trajectory in the s-pulse conditions; red lines, averaged trajectory in the p-pulse condition with ISI = 4 ms; blue lines, averaged trajectory in the p-pulse condition with ISI = 10 ms; gray lines, *x* and *y* variabilities (SEM, standard error of the mean) along the movement.

Results

Single-pulse TMS

Seminal works by Evarts (1968) and Georgopoulos et al. (1982) in the monkey, more recently confirmed in the human brain (Truccolo et al., 2008), showed that neurons in area M1 display different discharge rates, depending on the spatial position of the target (a phenomenon called "spatial tuning"), when planning and executing reaching movements. Here, in tasks in which participants planned visualized or memorized movements toward different spatial positions, we wanted to investigate whether MEPs (an index of corticospinal excitability) evoked by the TS in M1 are spatially tuned, as would be expected according to the

discharge of M1 neurons. Thus, we performed an ANOVA with the between-subject factor Task (Visually-guided vs Memory-guided) and with the within-subject factors Muscle (FDI vs ADM vs ECR vs FCR) and Position (right, left, far, near) with s-pulse MEPs as the dependent variable. This analysis revealed muscle-specific spatial tuning of MEP amplitude regardless of the Task, with significant interaction of Muscle with Position [$F_{(9,9)} = 4.03$, $p < 0.001$, partial $\eta^2 = 0.11$; Fig. 2, individual participant's data seen in Fig. 5*A*]. In particular, MEPs recorded from FDI muscle (Fig. 2, red lines) were significantly lower when planning to reach toward the near than toward the far ($p < 0.001$) and the left ($p = 0.004$) positions. The other comparisons were not significant ($p > 0.05$). MEPs recorded from ADM, ECR, and FCR were not spatially tuned (all $p > 0.29$).

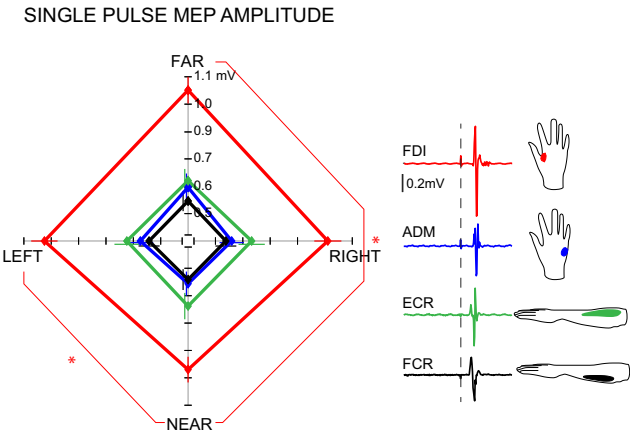

Figure 2. Single-pulse data. Left, Polar plot showing the amplitude of MEPs recorded from the FDI (red), ADM (blue), ECR (green), FCR (black) muscles during reach planning within the single-pulse conditions. FAR, Farther position, NEAR, nearer position, LEFT, left position, RIGHT, right position. Asterisks indicate significant *post hoc* comparisons ($p < 0.05$). The color of the asterisk indicates the muscle for which significant comparisons were found. Right, Exemplary MEPs recorded in each of the muscles, represented in the picture to the right. The vertical dashed line represents the time when the TMS pulse was delivered.

Paired-pulse effects

To investigate the effect that delivery of the CS over hV6A exerted on corticospinal excitability during motor planning, we calculated PPE, a measure of the ratio of MEP amplitudes between s-pulse and p-pulse. The calculation of PPE was conducted for each task, ISI, muscle, and position (see Materials and Methods), and we submitted them to an ANOVA with Task as the between-participants factor, and Muscle, ISI, and Position as within-participants factors.

We observed different effects of hV6A on corticospinal excitability according to the Muscle, to the Position, and to the ISI, but not to the Task. Specifically, PPE was affected by the main effect of Muscle ($F_{(3,3)} = 9.64$; Mauchly's sphericity test, $p < 0.001$; Huynh-Feldt adjusted, $p < 0.001$; partial $\eta^2 = 0.22$; Fig. 3*A*), driven by a stronger inhibition caused by CS over hV6A on the corticospinal excitability of FDI muscle than that of the other muscles (all $p < 0.002$), which in turn were not significantly different from each other (all $p = 1.00$). PPE was also influenced by the main effect of Position ($F_{(3,3)} = 3.01$; Mauchly's sphericity test, $p < 0.01$; Huynh-Feldt adjusted, $p < 0.04$; partial $\eta^2 = 0.08$), driven by the stronger inhibition during reach planning toward left positions ($p = 0.049$) than near positions (Fig. 3*B*). Moreover, PPE was also affected by the main effect of ISI ($F_{(1,1)} = 5.56$, $p = 0.02$, partial $\eta^2 = 0.14$) with lower PPE values for an ISI of 4 ms than for 10 ms (Fig. 3*C*). Neither effect of Task was significant (all $F < 0.1.65$, all $p > 0.10$, all partial $\eta^2 < 0.05$), nor were any other interaction effects.

To obtain a clearer view of the effects of hV6A on corticospinal excitability during reach planning, we evaluated the differences in PPE against zero (the null hypothesis of no effect of hV6A on M1) at each ISI, Muscle, and Position by pooling together the PPE of the two tasks, given the absence of task effect on the PPE mentioned above. The CS over hV6A inhibited corticospinal excitability, as demonstrated by the significantly negative PPE values: inhibitions were significant only with 4 ms ISIs in all muscles but with a position-specific trend (Fig. 4, individual participant's data, Fig. 5*B*). Significant inhibitions of MEPs of flexor muscles (Fig. 4*A*, FDI, *D*, FCR) were found only when planning to reach toward left positions (FDI: $t_{(35)} = -4.30$, $p < 0.001$; FCR: $t_{(35)} = -2.56$, $p = 0.01$) and right positions (FDI: $t_{(35)} = -4.43$, $p < 0.001$; FCR: $t_{(35)} = -2.56$, $p = 0.02$), which in turn were not statistically different (FDI: $F_{(1,35)} = 0.66$, partial $\eta^2 = 0.02$, $p = 0.42$; FCR: $F_{(1,35)} = 0.05$, partial $\eta^2 = 0.001$, $p = 0.83$).

The same trend was observed in the other muscles (Fig. 4*B*, ADM, Fig. 4*C*, ECR) when planning a movement toward left positions (ADM: $t_{(35)} = -2.24$, $p = 0.03$; ECR: $t_{(35)} = -2.52$, $p = 0.02$) and right positions (ADM: $t_{(35)} = -2.41$, $p = 0.02$; ECR: $t_{(35)} = -2.50$, $p = 0.02$). In ADM, we found an additional significant inhibition ($t_{(35)} = -2.27$, $p = 0.03$) during planning of far reaches. Inhibitions were not statistically different across positions

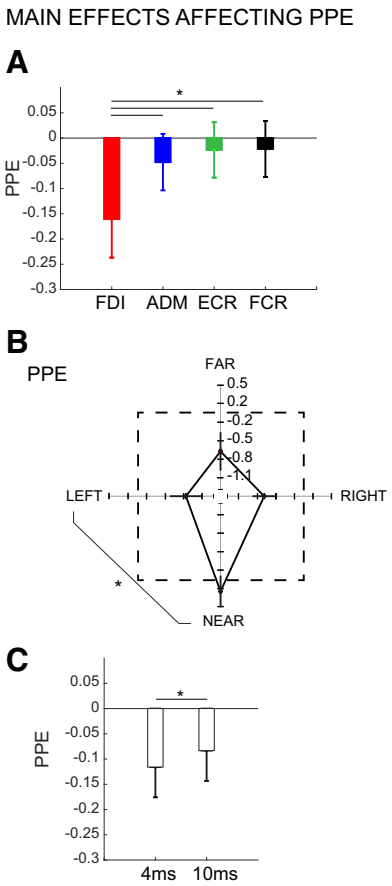

Figure 3. Main effects affecting PPE. ***A***, Main effect of the muscle is shown representing the changes in mean PPE across populations in each of the muscles tested. ***B***, Main effect of the position of the reaching target. ***C***, Main effect of ISI. Asterisks represent significant comparisons. Bars represent the SEM. Other conventions are as in Figures 1-2.

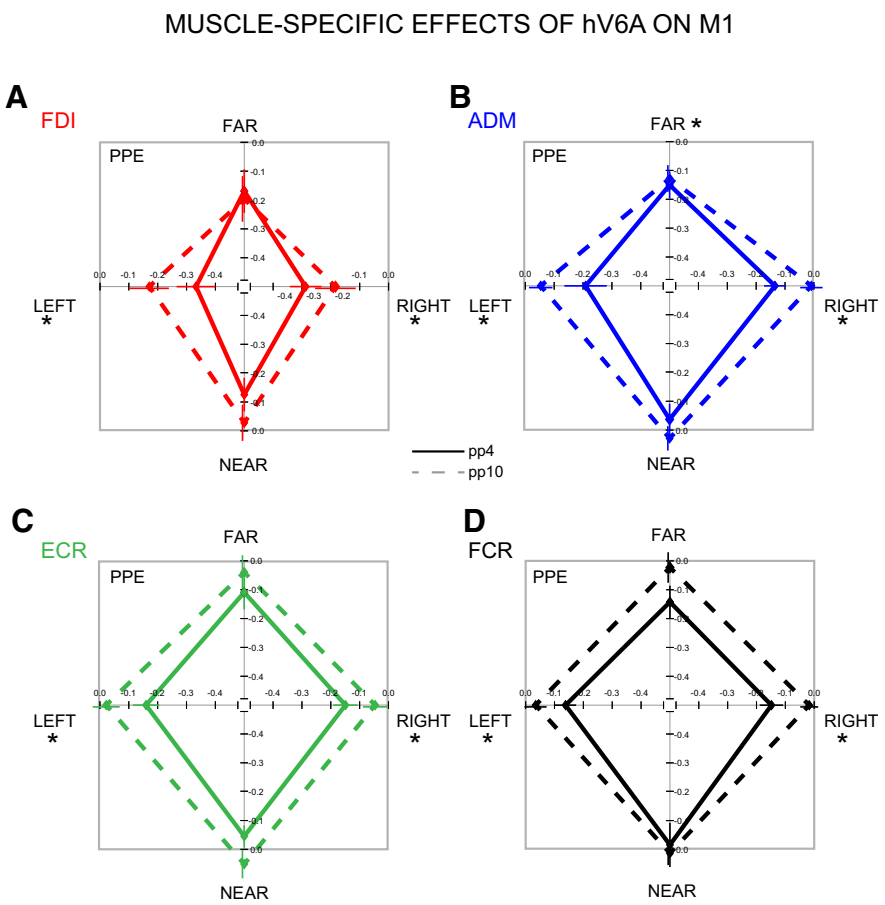

Figure 4. Effects of hV6A activity on corticospinal excitability in all muscles tested. ***A–D***, Polar plots represent the PPE values for the different muscles (***A***, FDI; ***B***, ADM; ***C***, ECR; ***D***, FCR), ISIs (continuous line, 4 ms; dashed line, 10 ms), and positions. Gray squares, PPE values of zero, which are indicative of no effect of hV6A on corticospinal excitability. Asterisks represent PPE values, which are significantly different from zero (one-sample *t* test, $p < 0.05$); therefore, marking positions in which hV6A exerted a significant modulation of corticospinal excitability. Conventions are as in Figures 1-2.

(ADM: $F_{(1,35)} = 0.66$, partial $\eta^2 = 0.02$, $p = 0.52$, ECR: $F_{(1,35)} = 0.04$, partial $\eta^2 = 0.001$, $p = 0.84$).

Reaction times were affected neither by the ISI (all $F < 1.81$, all $p > 0.17$, all partial $\eta^2 < 0.05$) nor by the Position ($F_{(3,105)} = 2.37$, $p = 0.07$, partial $\eta^2 = 0.06$). Thus, our TMS-induced effects on MEPs could not be accounted for by differences in reaction time.

In summary, during motor planning toward a visual or a memorized target, hV6A inhibited corticospinal excitability in all the muscles tested in a position-dependent manner when the CS was delivered 4 ms before the TS in M1. No effects were observed when the ISI was 10 ms. Corticospinal excitability during reach planning toward near positions, which showed the lowest MEP amplitude (Fig. 2), was never conditioned by hV6A, while left and right reach planning were the most affected in all the tested muscles.

MEP amplitude at rest

To investigate whether the execution of reaching affected corticospinal excitability at rest, we compared MEP amplitudes recorded at rest before and after reaching. No statistical differences were observed in any of the muscles (all $t < -1.33$, all $p > 0.19$). Moreover, no effects of tested ISIs (4 and 10 ms) were found (all $p > 0.35$, all $F < 1.08$, all $\eta^2 < 0.03$) in the resting blocks, in line with our recent work (Breveglieri et al., 2021b). A significant effect of Muscle was also found here ($F_{(3,105)} = 19.36$, partial $\eta^2 = 0.37$, $p < 0.001$), with a significantly higher MEP amplitude of FDI muscle than that recorded for other muscles (all $p < 0.001$).

Discussion

Correct functioning of the parieto-frontal circuits allows our spatial interactions with the environment to take place. We demonstrated here that corticospinal excitability is inhibited by hV6A during preparation of rightward and leftward reaching movements, as revealed by the significant suppression of MEPs and negative PPE values when CS was applied 4 ms before TS over the ipsilateral M1. This delivery of reach-related information from hV6A to M1 is compatible with monkey studies showing reach-related cells in monkey V6A (Fattori et al., 2005; Bosco et al., 2010; Hadjidimitrakis et al., 2014; Diomedi et al., 2021), as well as with fMRI activation in humans (Connolly et al., 2003; Prado et al., 2005; Fernandez-Ruiz et al., 2007; Filimon et al., 2009; Bernier and Grafton, 2010; Cavina-Pratesi et al., 2010) and with TMS studies (Koch et al., 2008; Vesia et al., 2013, 2017).

Spatial tuning of s-pulse MEPs

In the current study, the assessment of reach-related corticospinal excitability and parieto-frontal interactions was performed considering four muscles that are somehow involved in reaching, such as two finger muscles, FDI and ADM, and two extensor and flexor muscles of the wrist, ECR and FCR. In our study, participants were reaching toward targets located in different spatial positions, a design that enabled us to assess the spatial tuning of MEPs. When we delivered a single TS in area M1, MEPs recorded from FDI muscle were spatially tuned, whereas the MEPs recorded from the other muscles were not. The spatial tuning observed in FDI muscle is consistent with monkey studies (Evarts, 1968; Georgopoulos et al., 1982) showing that M1 cell discharges are spatially tuned. More recently, this result was confirmed in a single-cell study involving tetraplegic patients (Truccolo et al., 2008) who imagined reaches toward different positions. In this latter study, M1 neurons were tuned to the intended movement kinematics.

Only one of the recorded muscles (FDI) resulted as spatially tuned. The absence of spatial tuning of MEPs recorded from ADM, ECR, and FCR muscles could be explained considering that FDI muscle is an essential muscle for our pointing tasks, because the pointing was performed by the index finger, so this muscle is more sensitive than the others to pointing movements directed toward different spatial positions. The other muscles are less essential than FDI, being ADM specific for the little finger, and the ECR and FCR being specific for the wrist; thus, they are less involved in spatial aspects of pointing than the index finger.

Functional interactions hV6A–M1

An element of novelty of the current study is that we tested four different spatial positions here, located at different depths and

directions, whereas previous studies did not, because they focused on other aspects such as the comparison between reaching and grasping (Vesia et al., 2013) or compared different grasping actions (Vesia et al., 2017). We found a common frame of modulation of parieto-frontal interactions in the fingers and wrist muscles, since for all of these muscles excitability was reduced when planning leftward or rightward reaching. This supports the idea that the activation of the wrist and finger muscles involved in reach-to-point appear to involve common motor cortical circuits, in keeping with an fMRI study that shows an extensive overlap of wrist-related and finger-related activations (Sanes et al., 1995).

Interestingly, the feature of parieto-frontal interactions was independent of the task; that is, their functioning did not depend on the nature of motor planning. This means that the parieto-frontal interactions did not depend on the presence of visual information about the reaching target, so this flow of information may reflect reach goal representation instead of specific visuo-motor transformations. This is in keeping with the multiple features of reach-related cells of monkey V6A, which are modulated both in the light and in the dark (Bosco et al., 2010), and during reach planning to a visualized target (Fattori et al., 2005; Hadjidimitrakis et al., 2014; Diomedi et al., 2021) or a memorized target (Bosco et al., 2016). This is also in line with the similarity of the deficits observed in memory-guided compared with visually-guided reaching tasks following muscimol injections in a region located near the V6A in the monkey (Hwang et al., 2012).

Our results establish a causal transfer of directional, inhibitory information between regions of the parieto-frontal networks. This inhibition has been reported, specifically, when the CS over hV6A preceded the TS over M1 by 4 ms. This timing is the same as that which was effective in SPOC–M1 functional interactions during the planning of arm transport (Vesia et al., 2013) and is close to the timing that has been shown to be effective in lateral left PPC–M1 interactions (Koch et al., 2008) during reach planning. However, our results differ from those of Vesia et al. (2013) and Koch et al. (2008), because here we find inhibition of corticospinal excitability, whereas other studies found facilitatory interactions (Koch et al., 2008; Vesia et al., 2013).

This inhibition exerted by hV6A on M1 during reach planning, which is strongly compatible with the inhibitory-like neural signals conveyed by the premotor cortex to M1 (Civardi et al., 2001; Davare et al., 2008), might beneficially minimize the inertial consequences of the initial action on any alternative movement (Buch et al., 2010) that might be planned in parallel, and thus in competition (Cisek and Kalaska, 2010). Neurophysiological studies in humans have shown suppression of selected movement representations during response preparation (Hasbroucq et al., 1997, 1999; Davranche et al., 2007; Van Elswijk et al., 2007), named "impulse-control" (Duque and Ivry, 2009; Duque et al., 2010), which is presumably needed to prevent actions from being emitted prematurely. This effect is especially pronounced when the task requires the withholding of a selected action until the onset of an imperative signal (Boulinguez et al., 2008), such as when our participants withheld the planned action while waiting for the Go cue. This phenomenon may explain the difference between the excitations found in other studies (Koch et al., 2008; Vesia et al., 2013) and the inhibitions found here. Indeed, in the

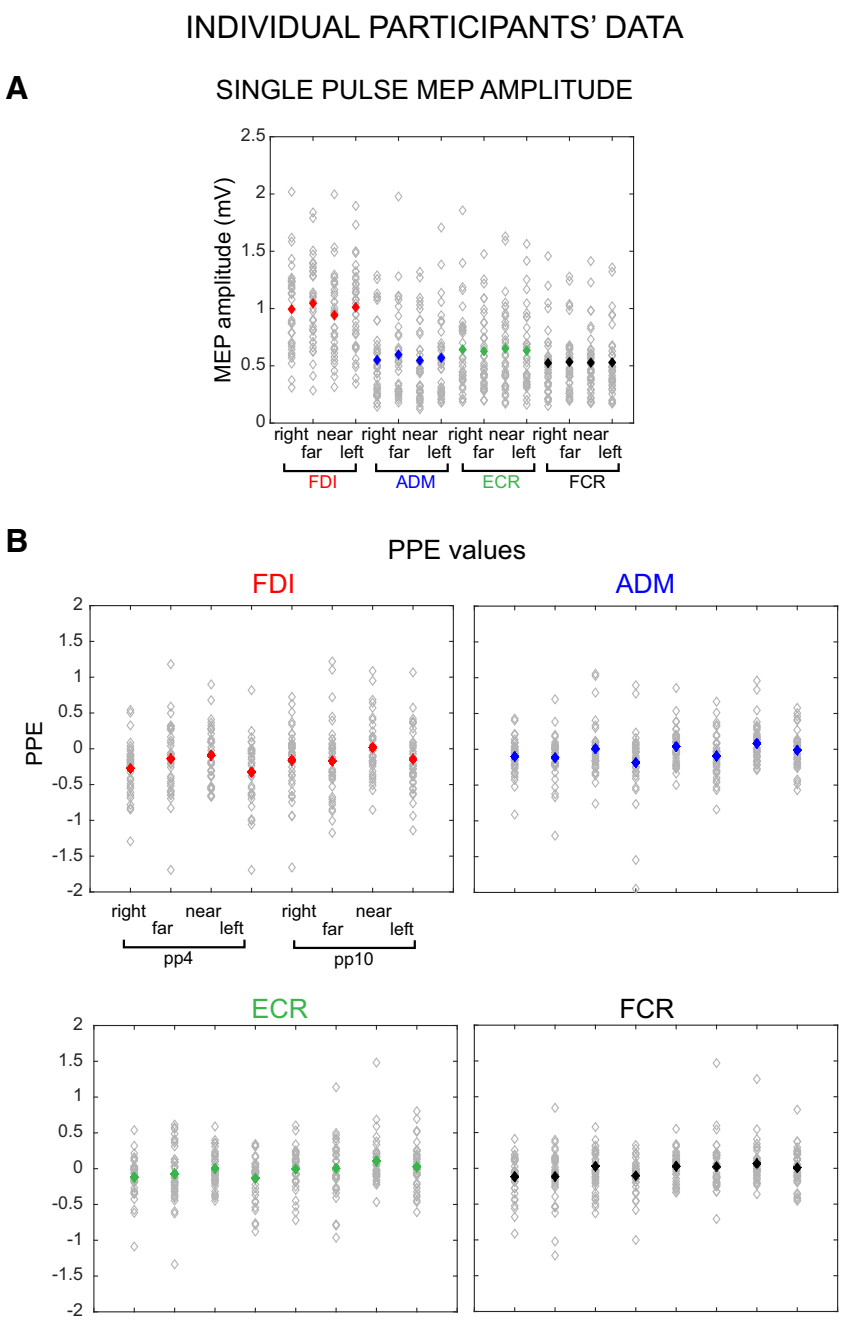

Figure 5. Data from individual participants. ***A***, ***B***, Empty gray diamonds represent the value of MEP amplitude (***A***) or the PPE value (***B***) of each individual participant, whereas filled diamonds represent mean data across the population. Other conventions are as in Figure 2-4.

experiment by Koch et al. (2008) the cue appearance was coincident with the Go signal, so the information about the spatial location to be reached was not withheld by the participants, which is different from our task. Furthermore, in the task of Vesia et al. (2013), the spatial location of the target was constant, so the cue was spatially uninformative, in contrast with the current study. These methodological differences may explain why we found inhibitory influences instead of excitatory ones (Koch et al., 2008; Vesia et al., 2013). Given that V6A in humans and monkeys is indirectly connected to M1 via the PMd (Gamberini et al., 2009; Tosoni et al., 2015), which is directly connected to M1, we suggest that the hV6A sends short-latency signals to the PMd, which sends inhibitory signals to M1 (Civardi et al., 2001), helping to control the execution of a selected response. Moreover, as PMd is also directly connected to the spinal cord (Dum and Strick, 1991), area V6A may play a role not only via M1, but also through PMd, directly on the spinal cord circuitry controlling motoneurons.

Short timing of interaction between V6A and M1

In this study, the effects of a CS over hV6A on the TS over M1 was specifically observed when ISI was 4 ms and not when ISI was 10 ms. This short timing of activation of the medial parieto-frontal networks during reach planning was different from the long-lasting effective timing (12–15 ms) that we recently observed at rest (Breveglieri et al., 2021b). This difference could be explained considering that the routes from the medial PPC to the frontal cortex are indirect and manifold. A shorter route includes the connections hV6A–PMd–M1, whereas a longer route involves hV6A–lateral PPC–PMv–M1 (Gamberini et al., 2009; Tosoni et al., 2015). The activation of these pathways may be dependent on the cognitive state, with the shorter route being exploited during reach planning and the longer route being used when at rest (Breveglieri et al., 2021b), a phenomenon also observed in other studies (Koch et al., 2006a, 2008; O'Shea et al., 2007; Davare et al., 2008; Mars et al., 2009; Buch et al., 2010, 2011; Neubert et al., 2010).

While it was reported that the modulation of parieto-frontal interactions is specific for the planning of contralateral reaching (Koch et al., 2008), here we show a bilateral modulation. This discrepancy could be ascribed to the difference in the stimulation sites between our study and that by Koch et al. (2008), our site being more medial than that used in the study by Koch et al. (2008). Indeed, it was suggested that medial PPC sites encode reach goals (Vesia et al., 2010, 2013), while more anterior-lateral sites reach vectors (Koch et al., 2008).

Conclusions

In conclusion, the short-latency inhibitory interactions between hV6A and M1 found here represent the functional support of the anatomic connections probed in humans with resting-state fMRI (Tosoni et al., 2015) and monkey hodological data (Gamberini et al., 2009), and claim for the functional homology between monkey and human mPPC.

References

Astafiev SV, Shulman GL, Stanley CM, Snyder AZ, Van Essen DC, Corbetta M (2003) Functional organization of human intraparietal and frontal cortex for attending, looking, and pointing. J Neurosci 23:4689–4699.

Bernier PM, Grafton ST (2010) Human posterior parietal cortex flexibly determines reference frames for reaching based on sensory context. Neuron 68:776–788.

Beurze SM, de Lange FP, Toni I, Medendorp WP (2009) Spatial and effector processing in the human parietofrontal network for reaches and saccades. J Neurophysiol 101:3053–3062.

Borgomaneri S, Vitale F, Avenanti A (2017) Behavioral inhibition system sensitivity enhances motor cortex suppression when watching fearful body expressions. Brain Struct Funct 222:3267–3282.

Bosco A, Breveglieri R, Chinellato E, Galletti C, Fattori P (2010) Reaching activity in the medial posterior parietal cortex of monkeys is modulated by visual feedback. J Neurosci 30:14773–14785.

Bosco A, Breveglieri R, Hadjidimitrakis K, Galletti C, Fattori P (2016) Reference frames for reaching when decoupling eye and target position in depth and direction. Sci Rep 6:21646.

Boulinguez P, Jaffard M, Granjon L, Benraiss A (2008) Warning signals induce automatic EMG activations and proactive volitional inhibition: evidence from analysis of error distribution in simple RT. J Neurophysiol 99:1572–1578.

Brainard DH (1997) The Psychophysics Toolbox. Spat Vis 10:433–436.

Breveglieri R, Bosco A, Borgomaneri S, Tessari A, Galletti C, Avenanti A, Fattori P (2021a) Transcranial magnetic stimulation over the human medial posterior parietal cortex disrupts depth encoding during reach planning. Cereb Cortex 31:267–280.

Breveglieri R, Borgomaneri S, Filippini M, De Vitis M, Tessari A, Fattori P (2021b) Functional connectivity at rest between the human medial posterior parietal cortex and the primary motor cortex detected by paired-pulse transcranial magnetic stimulation. Brain Sci 11:1357.

Buch ER, Mars RB, Boorman ED, Rushworth MFS (2010) A network centered on ventral premotor cortex exerts both facilitatory and inhibitory control over primary motor cortex during action reprogramming. J Neurosci 30:1395–1401.

Buch ER, Johnen VM, Nelissen N, O'Shea J, Rushworth MFS (2011) Noninvasive associative plasticity induction in a corticocortical pathway of the human brain. J Neurosci 31:17669–17679.

Cardellicchio P, Dolfini E, Fadiga L, D'Ausilio A (2020) Parallel fast and slow motor inhibition processes in joint action coordination. Cortex 133:346–357.

Carducci F, Brusco R (2012) Accuracy of an individualized MR-based head model for navigated brain stimulation. Psychiatry Res Neuroimaging 203:105–108.

Cavina-Pratesi C, Monaco S, Fattori P, Galletti C, McAdam TD, Quinlan DJ, Goodale MA, Culham JC (2010) Functional magnetic resonance imaging reveals the neural substrates of arm transport and grip formation in reach-to-grasp actions in humans. J Neurosci 30:10306–10323.

Chiappini E, Borgomaneri S, Marangon M, Turrini S, Romei V, Avenanti A (2020) Driving associative plasticity in premotor-motor connections through a novel paired associative stimulation based on long-latency cortico-cortical interactions. Brain Stimul 13:1461–1463.

Ciavarro M, Ambrosini E, Tosoni A, Committeri G, Fattori P, Galletti C (2013) rTMS of medial parieto-occipital cortex interferes with attentional reorienting during attention and reaching tasks. J Cogn Neurosci 25:1453–1462.

Cisek P, Kalaska JF (2010) Neural mechanisms for interacting with a world full of action choices. Annu Rev Neurosci 33:269–298.

Civardi C, Cantello R, Asselman P, Rothwell JC (2001) Transcranial magnetic stimulation can be used to test connections to primary motor areas from frontal and medial cortex in humans. Neuroimage 14:1444–1453.

Connolly JD, Andersen RA, Goodale MA (2003) FMRI evidence for a "parietal reach region" in the human brain. Exp Brain Res 153:140–145.

Davare M, Lemon R, Olivier E (2008) Selective modulation of interactions between ventral premotor cortex and primary motor cortex during precision grasping in humans. J Physiol 586:2735–2742.

Davranche K, Tandonnet C, Burle B, Meynier C, Vidal F, Hasbroucq T (2007) The dual nature of time preparation: neural activation and suppression revealed by transcranial magnetic stimulation of the motor cortex. Eur J Neurosci 25:3766–3774.

Diomedi S, Vaccari FE, Filippini M, Fattori P, Galletti C (2020) Mixed selectivity in macaque medial parietal cortex during eye-hand reaching. iScience 23:101616.

Diomedi S, Vaccari FE, Galletti C, Hadjidimitrakis K, Fattori P (2021) Motor-like neural dynamics in two parietal areas during arm reaching. Prog Neurobiol 205:102116.

Dum RP, Strick PL (1991) The origin of corticospinal projections from the premotor areas in the frontal lobe. J Neurosci 11:667–689.
Duque J, Ivry RB (2009) Role of corticospinal suppression during motor preparation. Cereb Cortex 19:2013–2024.
Duque J, Lew D, Mazzocchio R, Olivier E, Ivry RB (2010) Evidence for two concurrent inhibitory mechanisms during response preparation. J Neurosci 30:3793–3802.
Evarts EV (1968) Relation of pyramidal tract activity to force exerted during voluntary movement. J Neurophysiol 31:14–27.
Fattori P, Kutz DF, Breveglieri R, Marzocchi N, Galletti C (2005) Spatial tuning of reaching activity in the medial parieto-occipital cortex (area V6A) of macaque monkey. Eur J Neurosci 22:956–972.
Fattori P, Breveglieri R, Bosco A, Gamberini M, Galletti C (2017) Vision for prehension in the medial parietal cortex. Cereb Cortex 27:1149–1163.
Faul F, Erdfelder E, Lang A, Buchner A (2007) G*Power 3: a flexible statistical power analysis program for the social, behavioral, and biomedical sciences. Behav Res Methods 39:175–191.
Fernandez-Ruiz J, Goltz HC, DeSouza JFX, Vilis T, Crawford JD (2007) Human parietal "reach region" primarily encodes intrinsic visual direction, not extrinsic movement direction, in a visual-motor dissociation task. Cereb Cortex 17:2283–2292.
Filimon F, Nelson JD, Huang RS, Sereno MI (2009) Multiple parietal reach regions in humans: cortical representations for visual and proprioceptive feedback during on-line reaching. J Neurosci 29:2961–2971.
Fiori F, Chiappini E, Soriano M, Paracampo R, Romei V, Borgomaneri S, Avenanti A (2016) Long-latency modulation of motor cortex excitability by ipsilateral posterior inferior frontal gyrus and pre-supplementary motor area. Sci Rep 6:38396.
Fiori F, Chiappini E, Candidi M, Romei V, Borgomaneri S, Avenanti A (2017) Long-latency interhemispheric interactions between motor-related areas and the primary motor cortex: a dual site TMS study. Sci Rep 7:14936.
Galletti C, Fattori P, Kutz DF, Gamberini M (1999) Brain location and visual topography of cortical area V6A in the macaque monkey. Eur J Neurosci 11:575–582.
Galletti C, Fattori P, Gamberini M, Kutz D (2004) The most direct visual pathway to the frontal cortex. Cortex 40:216–217.
Gallivan JP, McLean A, Culham JC (2011) Neuroimaging reveals enhanced activation in a reach-selective brain area for objects located within participants' typical hand workspaces. Neuropsychologia 49: 3710–3721.
Gamberini M, Passarelli L, Fattori P, Zucchelli M, Bakola S, Luppino G, Galletti C (2009) Cortical connections of the visuomotor parietooccipital area V6Ad of the macaque monkey. J Comp Neurol 513: 622–642.
Georgopoulos AP, Kalaska JF, Caminiti R, Massey JT (1982) On the relations between the direction of two-dimensional arm movements and cell discharge in primate motor cortex. J Neurosci 2:1527–1537.
Hadjidimitrakis K, Bertozzi F, Breveglieri R, Bosco A, Galletti C, Fattori P (2014) Common neural substrate for processing depth and direction signals for reaching in the monkey medial posterior parietal cortex. Cereb Cortex 24:1645–1657.
Hasbroucq T, Kaneko H, Akamatsu M, Possamai CA (1997) Preparatory inhibition of cortico-spinal excitability: a transcranial magnetic stimulation study in man. Brain Res Cogn Brain Res 5:185–192.
Hasbroucq T, Kaneko H, Akamatsu M, Possamai CA (1999) The time course of preparatory spinal and cortico-spinal inhibition: an H-reflex and transcranial magnetic stimulation study in man. Exp Brain Res 124:33–41.
Hwang EJ, Hauschild M, Wilke M, Andersen RA (2012) Inactivation of the parietal reach region causes optic ataxia, impairing reaches but not saccades. Neuron 76:1021–1029.
Koch G, Franca M, Albrecht UV, Caltagirone C, Rothwell JC (2006a) Effects of paired pulse TMS of primary somatosensory cortex on perception of a peripheral electrical stimulus. Exp Brain Res 172:416–424.
Koch G, Franca M, Mochizuchi H, Marconi B, Caltagirone C, Rothwell JC (2006b) Interactions between pairs of transcranial magnetic stimuli over the human left dorsal premotor cortex differ from those seen in primary motor cortex. J Physiol 578:551–562.
Koch G, Del Olmo MF, Cheeran B, Ruge D, Schippling S, Caltagirone C, Rothwell JC (2007) Focal stimulation of the posterior parietal cortex increases the excitability of the ipsilateral motor cortex. J Neurosci 27:6815–6822.
Koch G, D, Olmo MF, Cheeran B, Schippling S, Caltagirone C, Driver J, Rothwell JC (2008) Functional interplay between posterior parietal and ipsilateral motor cortex revealed by twin-coil transcranial magnetic stimulation during reach planning toward contralateral space. J Neurosci 28:5944–5953.
Mars RB, Klein MC, Neubert FX, Olivier E, Buch ER, Boorman ED, Rushworth MF (2009) Short-latency influence of medial frontal cortex on primary motor cortex during action selection under conflict. J Neurosci 29:6926–6931.
Mountcastle VB, Lynch JC, Georgopoulos G, Sakata H, Acuna C (1975) Posterior parietal association cortex of the monkey: command functions for operations within extrapersonal space. J Neurophysiol 38:871–908.
Neubert F-X, Mars RB, Buch ER, Olivier E, Rushworth MFS (2010) Cortical and subcortical interactions during action reprogramming and their related white matter pathways. Proc Natl Acad Sci U S A 107:13240–13245.
O'Shea J, Sebastian C, Boorman ED, Johansen-Berg H, Rushworth MFS (2007) Functional specificity of human premotor-motor cortical interactions during action selection. Eur J Neurosci 26:2085–2095.
Oldfield RC (1971) The assessment and analysis of handedness: the Edinburgh inventory. Neuropsychologia 9:97–113.
Passarelli L, Rosa MGP, Gamberini M, Bakola S, Burman KJ, Fattori P, Galletti C (2011) Cortical connections of area V6Av in the macaque: a visual-input node to the eye/hand coordination system. J Neurosci 31:1790–1801.
Passarelli L, Rosa MGP, Bakola S, Gamberini M, Worthy KH, Fattori P, Galletti C (2018) Uniformity and diversity of cortical projections to precuneate areas in the macaque monkey: what defines area PGm? Cereb Cortex 28:1700–1717.
Pitzalis S, Sereno MI, Committeri G, Fattori P, Galati G, Tosoni A, Galletti C (2013) The human homologue of macaque area V6A. Neuroimage 82:517–530.
Pitzalis S, Fattori P, Galletti C (2015) The human cortical areas V6 and V6A. Vis Neurosci 32:E007.
Prado J, Clavagnier S, Otzenberger H, Scheiber C, Kennedy H, Perenin MT (2005) Two cortical systems for reaching in central and peripheral vision. Neuron 48:849–858.
Rossi S, Hallett M, Rossini PM, Pascual-Leone A (2009) Safety, ethical considerations, and application guidelines for the use of transcranial magnetic stimulation in clinical practice and research. Clin Neurophysiol 120:2008–2039.
Rossini PM, et al. (2015) Non-invasive electrical and magnetic stimulation of the brain, spinal cord, roots and peripheral nerves: basic principles and procedures for routine clinical and research application. An updated report from an I.F.C.N. Committee. Clin Neurophysiol 126:1071–1107.
Rothwell JC (2011) Using transcranial magnetic stimulation methods to probe connectivity between motor areas of the brain. Hum Mov Sci 30:906–915.
Sanes JN, Donoghue JP, Thangaraj V, Edelman RR, Warach S (1995) Shared neural substrates controlling hand movements in human motor cortex. Science 268:1775–1777.
Snyder LH, Batista AP, Andersen RA (2000) Intention-related activity in the posterior parietal cortex: a review. Vision Res 40:1433–1441.
Talairach J, Tournoux P (1988) Co-planar stereotaxic atlas of the human brain: 3-dimensional proportional system: an approach to cerebral imaging. Stuttgart, NY: Thieme Medical.
Tosoni A, Pitzalis S, Committeri G, Fattori P, Galletti C, Galati G (2015) Resting-state connectivity and functional specialization in human medial parieto-occipital cortex. Brain Struct Funct 220: 3307–3321.
Truccolo W, Friehs GM, Donoghue JP, Hochberg LR (2008) Primary motor cortex tuning to intended movement kinematics in humans with tetraplegia. J Neurosci 28:1163–1178.
Van Campen AD, Neubert FX, Van Den Wildenberg WPM, Riddenrinkhof KR, Mars RB (2013) Paired-pulse transcranial magnetic stimulation reveals probability-dependent changes in functional connectivity between right inferior frontal cortex and primary motor cortex during go/no-go performance. Front Hum Neurosci 7:736.

Van Elswijk G, Kleine BU, Overeem S, Stegeman DF (2007) Expectancy induces dynamic modulation of corticospinal excitability. J Cogni Neurosci 19:121–131.

Vesia M, Monteon JA, Sergio LE, Crawford JD (2006) Hemispheric asymmetry in memory-guided pointing during single-pulse transcranial magnetic stimulation of human parietal cortex. J Neurophysiol 96:3016–3027.

Vesia M, Yan X, Henriques DY, Sergio LE, Crawford JD (2008) Transcranial magnetic stimulation over human dorsal-lateral posterior parietal cortex disrupts integration of hand position signals into the reach plan. J Neurophysiol 100:2005–2014.

Vesia M, Prime SL, Yan X, Sergio LE, Crawford JD (2010) Specificity of human parietal saccade and reach regions during transcranial magnetic stimulation. J Neurosci 30:13053–13065.

Vesia M, Bolton DA, Mochizuki G, Staines WR (2013) Human parietal and primary motor cortical interactions are selectively modulated during the transport and grip formation of goal-directed hand actions. Neuropsychologia 51:410–417.

Vesia M, Barnett-Cowan M, Elahi B, Jegatheeswaran G, Isayama R, Neva JL, Davare M, Staines WR, Culham JC, Chen R (2017) Human dorsomedial parieto-motor circuit specifies grasp during the planning of goal-directed hand actions. Cortex 92:175–186.